LASER INTERFEROMETER GRAVITATIONAL WAVE OBSERVATORY
- LIGO -
CALIFORNIA INSTITUTE OF TECHNOLOGY
MASSACHUSETTS INSTITUTE OF TECHNOLOGY

Technical Note	**LIGO-T080074-00-R**	2008/04/17

Upgrade of the 40M Interferometer

R. Adhikari, Y. Aso, S. Ballmer, R. Bork, J. Miller, S. Vass, R. Ward, A. Weinstein

Distribution of this document:

ISC Group

California Institute of Technology
LIGO Project, MS 18-34
Pasadena, CA 91125
Phone (626) 395-2129
Fax (626) 304-9834
E-mail: info@ligo.caltech.edu

Massachusetts Institute of Technology
LIGO Project, Room NW22-295
Cambridge, MA 02139
Phone (617) 253-4824
Fax (617) 253-7014
E-mail: info@ligo.mit.edu

LIGO Hanford Observatory
Route 10, Mile Marker 2
Richland, WA 99352
Phone (509) 372-8106
Fax (509) 372-8137
E-mail: info@ligo.caltech.edu

LIGO Livingston Observatory
19100 LIGO Lane
Livingston, LA 70754
Phone (225) 686-3100
Fax (225) 686-7189
E-mail: info@ligo.caltech.edu

http://www.ligo.caltech.edu/

1 Overview

This document describes the proposed upgrade of the 40m prototype interferometer at Caltech. Detailed background and motivation is given in Appendix D.

The purpose of the upgrade is to match the properties of the 40m interferometer to the recent design of the Advanced LIGO interferometer [3] (T070247-00) and to enable more faithful prototyping of the real thing.

The following is a list of the major changes:

- Arm Cavity Finesse. The ITM transmission will be changed to match the AdvLIGO finesse choice of 450 (T = 1.4%)
- Lightweight ITMs. In order to increase the effects of radiation pressure we will replace the 1.25 kg MOS's with the 0.25 kg SOSs.
- Modulation Frequencies. The 40m frequencies ($f_1 = 33$ MHz and $f_2 = 166$ MHz) will be changed to match the AdvLIGO frequencies ($f_1 = 9$ MHz and $f_2 = 45$ MHz).
- Recycling Cavities. The PRC and SRC will be made longer to accommodate the lower modulation frequencies. This will be done by folding the cavities using passively damped ANU tip/tilt suspended optics.
- Mach Zehnder. The CDD shows that it is not necessary to have a Mach Zucker so we will remove the 40m Mach Zucker and go back to using serial modulation.
- Controls Computers. All of the front end processors, ADCs, and DACs will be replaced with AdvLIGO style hardware. There will be one or two central multi-core computers with fiber links to remote ADC/DAC "blue-boxes". Custom interface connectors will be made to connect the new digital controls with the existing analog electronics.
- Multi wavelength locking. Investigate techniques to improve mean time to lock: Multi-wavelength locking locking using dichroic optics (green, blue), frequency shifted PSL light injected through ETM or pick-off ports, PRN techniques.
- Optical Levers. Test out fiber based OL distribution scheme? Not really necessary. We should make sure to include whitening of all Oplev systems.
- Wavefront Sensing. The 40m will continue to only have wavefront sensing for the IMC. The full interferometer alignment will continue to be done by angular dither demodulation.
- Adaptive Noise Cancellation. There will be a few adaptive noise cancellation machines to study the technique. This will require some new computers, PEM sensors, shakers, etc.

2 Descriptions of the Changes

2.1 Modulation Frequencies

The current modulation frequencies for the main interferometer are (f_1 = 33 MHz & f_2= 166 MHz). The modulation frequency for the input mode cleaner is (f_{MC} = 29.5 MHz). There are many practical difficulties associated with using such high frequencies: small photodiodes to reduce diode capacitance, increased dielectric losses in the RF cables, incompatibility with the existing RF board layouts, and incompatibility with the LIGO standard op-amp collection.

This experience led to a design choice (f_1 = 9 MHz and f_2 = 45 MHz) for Advanced LIGO utilizing a much lower frequency pair than the previous design (f_1 = 9 MHz and f_2 = 180 MHz).

2.2 Recycling Cavity Lengths

The recycling cavity lengths will be made much longer than is current (see Tables 4 and 5). This will require the installation of 2 folding mirrors per cavity. Since the 40m stacks do not give much seismic isolation in the control band (reference?) we have chosen to install a variant of the ANU Tip-Tilt mirrors to provide some isolation. In order to not have the added complexity of controlling 4 more suspended optics, we will take advantage of the inherent eddy current damping in the cages (reference - add tip/tilt plots). We will also not install BOSEMs or coils in these. They will be passively damped, uncontrolled folding mirrors. The residual excitation at the Tip-Tilt free body modes is small (the Q is 2). Some basic Looptickle modeling shows that the 1/f isolation provided by the Tip-Tilt mirrors is enough to bring the noise from the recycling cavities to a level where it is below the thermal noise in the arm cavity suspensions.

Figure 1 and 2 show two possible layouts for the recycling cavities that are consistent with the cavity length requirements (see section 3).

2.3 Mode Cleaner

It will be made longer. The existing Input Mode Cleaner (IMC) length is 13.548 m [14] and is resonant with an 11.064 MHz RF sideband. The new length will be 16.65 m, requiring a 3.1 m extension. This can be accommodated in the 40m lab (see figure **??**) by installing an extension tube between the existing tube and the MC2 chamber. This is expected to be a fairly simple operation.

We would have qualitatively the same prototyping experience whether we used a 9 or 11 MHz sideband but since it is relatively easy and inexpensive we feel that it is worth it to use the exact frequencies in case there is something surprising to be learned about components, RFI, etc.

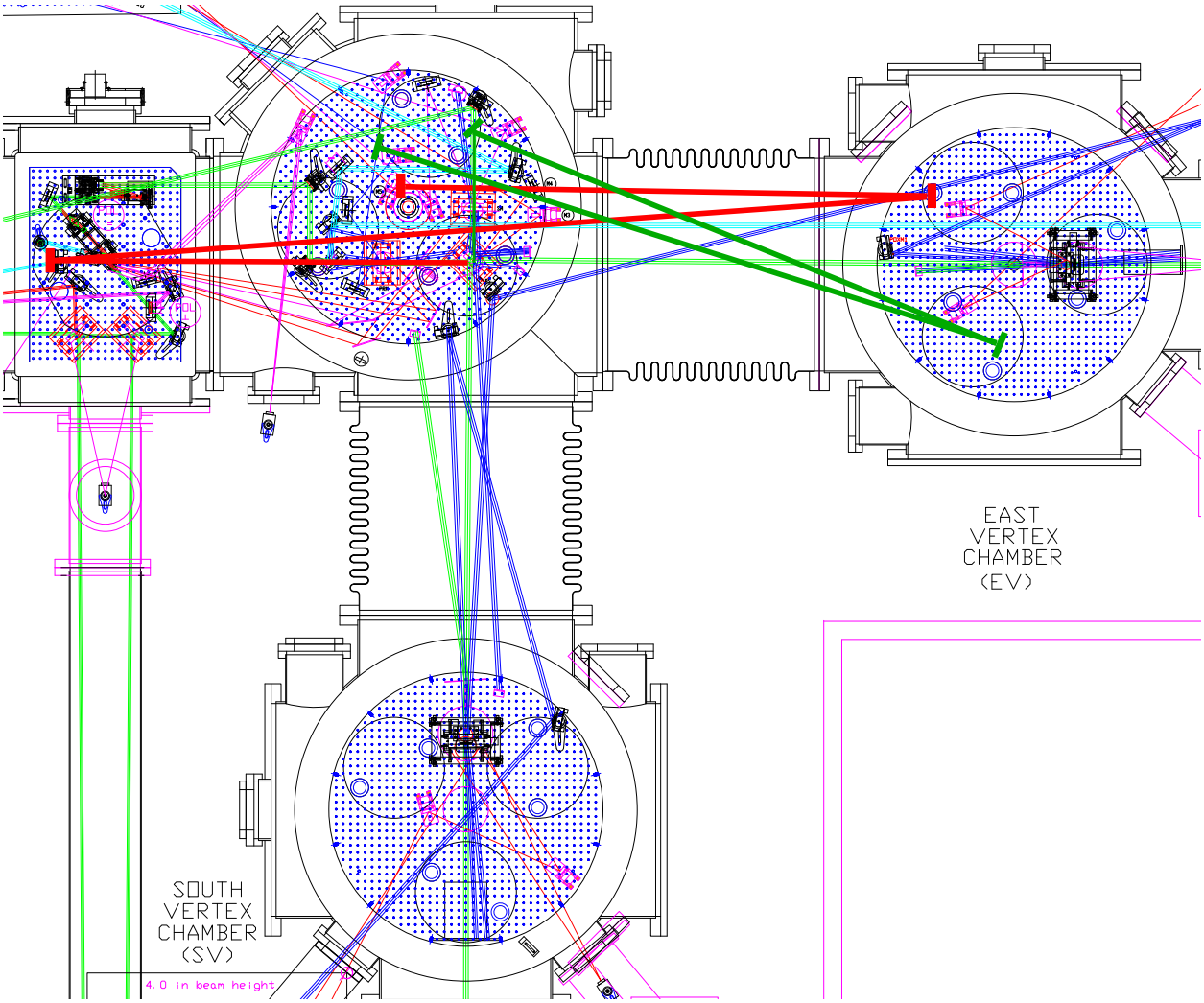

Figure 1: Possible way to fold both recycling cavities with 2 folding mirrors per cavity. The power recycling cavity is shown in red, the signal recycling cavity in green.

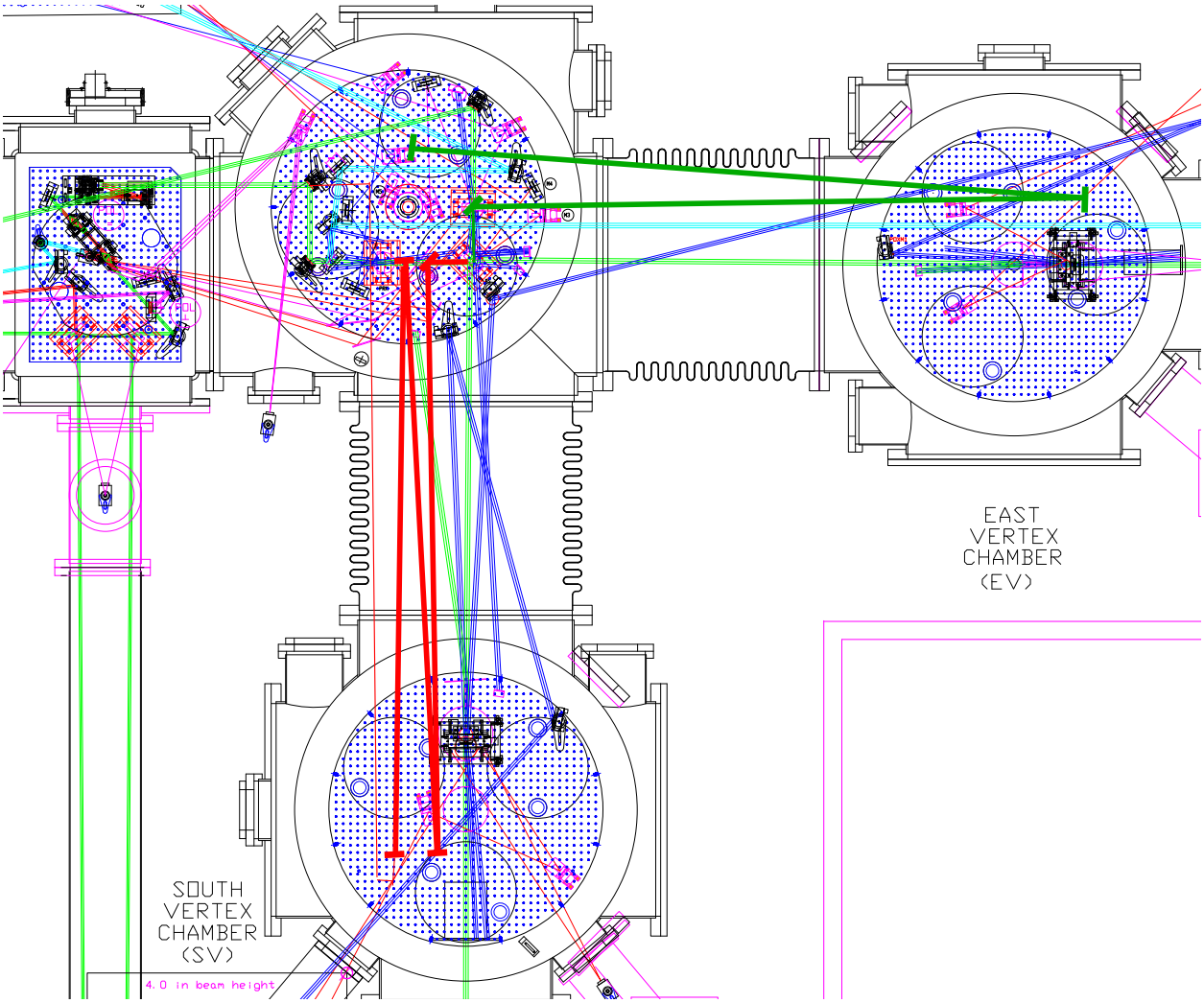

Figure 2: Possible way to fold both recycling cavities with 3 folding mirrors for the power cavity. The power cavity is shown in red, the signal cavity in green.

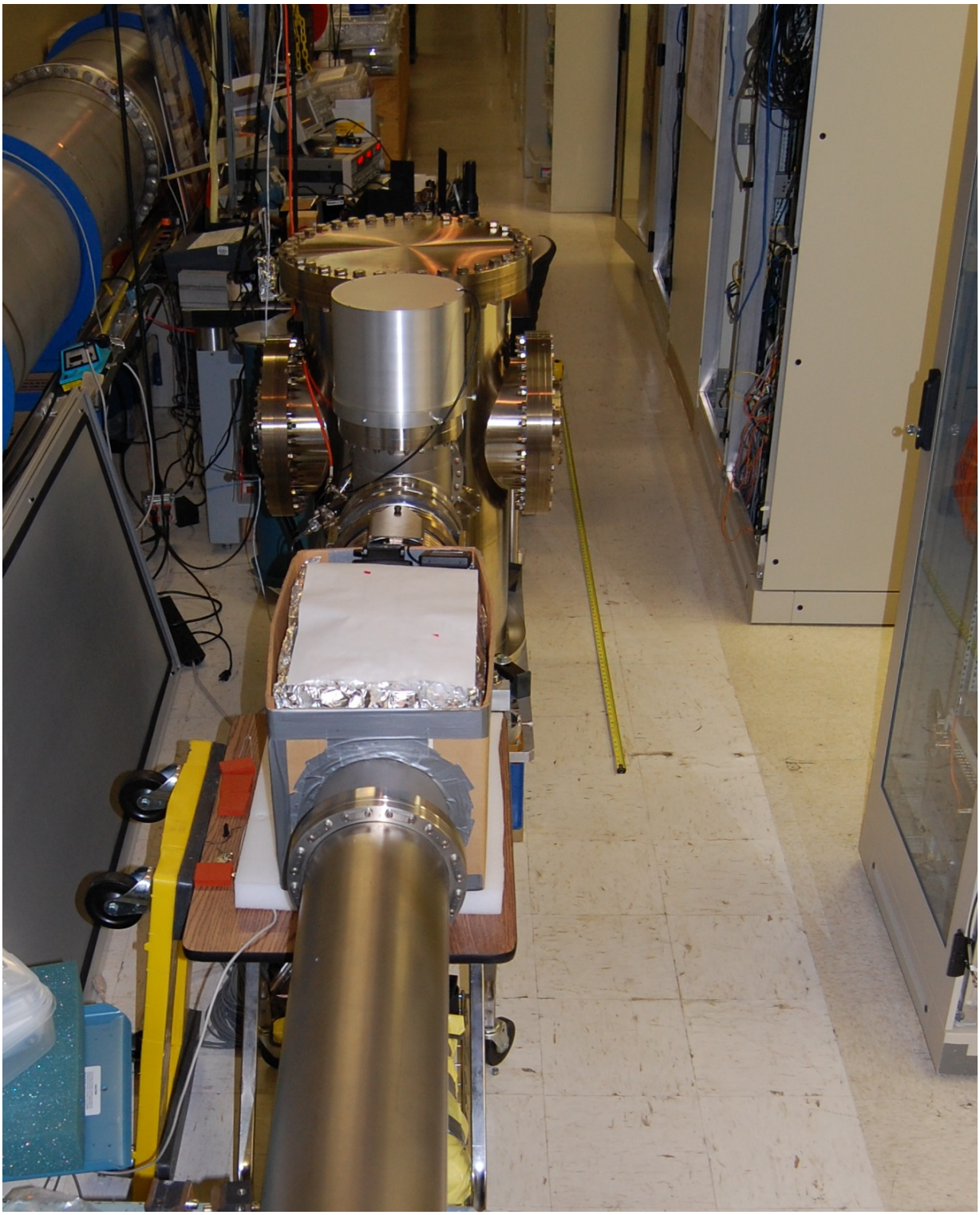

Figure 3: View of the MC2 tank from around the MC1 chamber.

2.4 Arm Cavity Finesse

The arm cavity finesse will be changed from 1200 to 450 to match the new design [4]. This will require repolishing and recoating the ITMs. We place no requirements on the thermal noise or the polish and so we can afford to go with the cheapest / fastest vendors (within reason). For the coating, we will require the transmission of the ITM HR surface to be 0.014 +/- 0.002 and that the differential transmission (T_X - T_Y) be less than 0.001. This is to prevent there being excess noise couplings which are qualitatively beyond what we expect in Advanced LIGO.

2.5 ITM Masses

For the new ITMs we have the choice of either installing 2 MOSs or 2 SOSs.

There are 2 ITM MOS spares on hand and more than enough MCFM spares that we can choose between them.

Installing SOSs will increase the effect of radiation pressure and therefore require developing controls techniques which will be useful in Advanced LIGO. We estimate that with SOS-ITMs, the longitudinal optical spring can be made as high as 200 Hz in the detuned RSE case. This seems, at this stage, like a potentially useful thing to prototype and so we are planning to install SOS ITMs.

2.6 Borkspace Revolution

The current CPU power for the SUS and LSC FEs is undersized at the 40m. These processors frequently run over their time limit and fall out of sync, requiring reboots of several systems. We therefore would like to replace several of these with a single multi-core computer (Sun Fire X4600 M2 AMD; 8 x 2.8 GHz Dual Core Opteron). Changing from the VME crate style Pentiums to the commodity FE processor will make the upgrade path easier in the future. There is also the significant benefit of producing ~7 spare VME processors for the observatories during the Enhanced LIGO science runs.

We should put a table in here of all the FE computers, what they are, how much time they take up, and how many ADC/DAC connections they have, and how many signals they pass to where across the RFM net.

Figure 8 shows an example block diagram of what would be prototyped at the 40m lab. This is also the proposed new DAQ structure for Enhanced LIGO.

2.7 Wavefront Sensing

The 40m is the only place outside of the actual Advanced LIGO interferometers that the full ASC-WFS system could be prototyped. The iLIGO experience was difficult because of difficult to diagnose problems in the WFS heads, demod boards, whitening boards, and ADCs. On the optical side the WFS sensing matrix was often degenerate and singular due to ill understood properties of the unstable power recycling cavity and the Sigg-Sidles torque instabilities.

It will certainly be valuable to test out the full electronics chain with realistic optical signals but the 40m optical plant is unlikely to be a good prototype of the Advanced LIGO interferometer since the 40m arms will not be changed to approach the nearly unstable, confocal geometry of Advanced LIGO.

Unless something unforeseen comes up, we will simply make the 40m available as a lab to test the WFS electronics chain if it proves to be convenient (e.g. by installing an Advanced LIGO WFS system on the IMC). We will not setup a full IFO RF WFS system.

On the other hand, we will continue to commission the dither based alignment system so as to have a useful bootstrap system when commissioning the WFS in Advanced LIGO.

2.8 Optical Levers

Currently the 40m optical lever system serves to stablize the low frequency (¡ 6 Hz) motion of the suspended optics. The lever lengths are 1-3 meters long and use HeNe lasers. Due to geometrical constraints the beams bounce off of fixed mirrors on the stacks on the input and output paths. It is clear that the sensing noise of the system is limited by bouncing off of the stack (f ¡ 10 Hz) and from a lack of whitening before the ADCs (f ¿ 10 Hz).

The new design will use existing viewports, port mounted steering mirrors, and simple telescopes with 2 inch optics to make 40m long optical levers.

3 Looptickle Modeling

This section contains the results from a Looptickle / Optickle model. It focuses on the zero-detuned mode that is going to be the main mode of AdvLIGO.

3.1 Design parameters

Table 1 summarizes the key design parameters. All cavity length are optical path length numbers, i.e. they have not been corrected for the BS thickness.

3.2 Loop Designs

No magic in this section. we aimed for a DARM UGF of 350 Hz, and auxiliary loop UGF's of 100 Hz. But neither of them are critical.

3.3 Power / Signal Levels

The table below shows the optical power at each port. No additional attenuators were included. The POP beam assumes a PRC folding mirror with 1000 ppm transmission. A DARM offset of 40 pm was assumed. This gives 1.5 mWatt of power on the DC detector. The offset can be increased more, but the sensitivity will go down.

Quantity	*Value*
Input power	1 Watt
Finesse	446
ITM transmission	0.014
PRM transmission (unchanged)	0.07
SRM transmission (unchanged)	0.07
Schnupp asymmetry	0.050
l_{PRC}	8.328 m
l_{SRC}	6.662 m
Distance BS to ITMX	2.025 m
Distance BS to ITMY	1.975 m
Distance BS to PRM	6.328 m
Distance BS to SRM	4.662 m
l_{IMC} (round trip)	33.310 m
l_{EX}	38.55 m
l_{EY}	38.55 m
Lower mod. frequency	9 MHz
Upper mod. frequency	45 MHz

Table 1: Basic interferometer parameters.

Optical Port Power in mWatt

FREQ (MHz)	-54.0	-45.0	-36.0	-28.8	-9.0	0.0	9.0	28.8	36.0	45.0	54.0	Total
REFL	0.0	0.2	0.0	0.0	2.0	26.8	2.0	0.0	0.0	0.2	0.0	31.2
AS	0.0	0.0	0.0	0.0	0.0	1.5	0.0	0.0	0.0	0.0	0.0	1.5
POP	0.0	0.0	0.0	0.0	0.1	17.6	0.1	0.0	0.0	0.0	0.0	17.9

And the following table shows the RF power at each port in mWatt (both quadratures).

RF power at ports in mWatt

FREQ (MHz)	0.0	9.0	18.0	36.0	45.0	54.0	90.0
REFL	31.17	0.02	4.01	0.82	0.01	0.83	0.35
AS	1.48	0.01	0.00	0.00	0.11	0.00	0.00
POP2	17.91	0.00	0.24	0.19	0.00	0.19	0.03

3.4 Noise Subtraction

Since the suspension thermal noise is dominant, we only need a modest amount of MICH subtraction to suppress the MICH noise below thermal noise. However, the couplings are the same as for AdvLIGO, and there is no reason not to implement the same subtractions.

3.5 DARM Noise Budget

The Looptickle model included the following noise sources:

- **Quantum** or **Shot Noise** from the loop itself, calculated by injecting vacuum noise at every open optical port.
- **Auxiliary length**: Shot Noise from the other loops, calculated by propagating the quantum noise in the other loops through the control system.
- **Seismic Noise**, This is an estimate (power law) for the noise at the 40m. It includes coupling through the new Eddy-current damped recycling cavity folding mirrors.
- **Mirror Thermal** noise, estimate for 40m.
- **Suspension Thermal** noise, estimate for 40m.
- **Frequency Noise** incident on the input mode cleaner (i.e. input mode cleaner and common mode sensing noise are counted as shot noise from those length loops). See figure 5 for the assumed PSL noise level.
- **Intensity Noise** incident on the IMC. The measured out-of-loop noise from the 40m ISS is 3×10^{-8} from 80-3000 Hz. See figure 5 for the assumed PSL noise level.
- **Oscillator Phase Noise**. See figure 5 for the assumed PSL noise level. The coupling does include the light passing through the IMC. Currently the estimate does not include potential noise added after the EOM/LO split. The 40m lab currently uses IFR (Marconi) 2023 generators instead of Wenzel crystals for signal generation.
- **Oscillator Amplitude Noise** See figure 5 for the assumed PSL noise level. Measurements of the iLIGO RF AM Stabilization box at the 40m [15] show that the AM noise stabilized EOM drive can be as low as $5 \times 10^{-8}/\sqrt{\text{Hz}}$ above 10 Hz.

Figure 4 shows a noise budget for DARM.

3.6 Optickle Sensing Matrices

Tables 3.6 and 3.6 show the full sensing matrix at 100 Hz and 1 kHz. We intend to used the same error signals as AdvLIGO, namely REFL_I1 for CARM, AS_DC for DARM, POP_I1 for PRCL, POP_Q2 for MICH and POP_I2 for SRCL. The 3-f signals for lock acquisition are easy to add, but were not yet modeled.

4 Lock Acquisition

The duration of the lock acquisition process should be short enough to not significantly impact the Detector availability for science mode operation. In Acquisition mode there are no requirements on the noise in the sensing systems (length or angle) in the GW band other than what is required to prevent saturations during acquisition.

The low frequency (control band) angular fluctuations must be consistent with small gain fluctuations in all LSC and ISC loops.

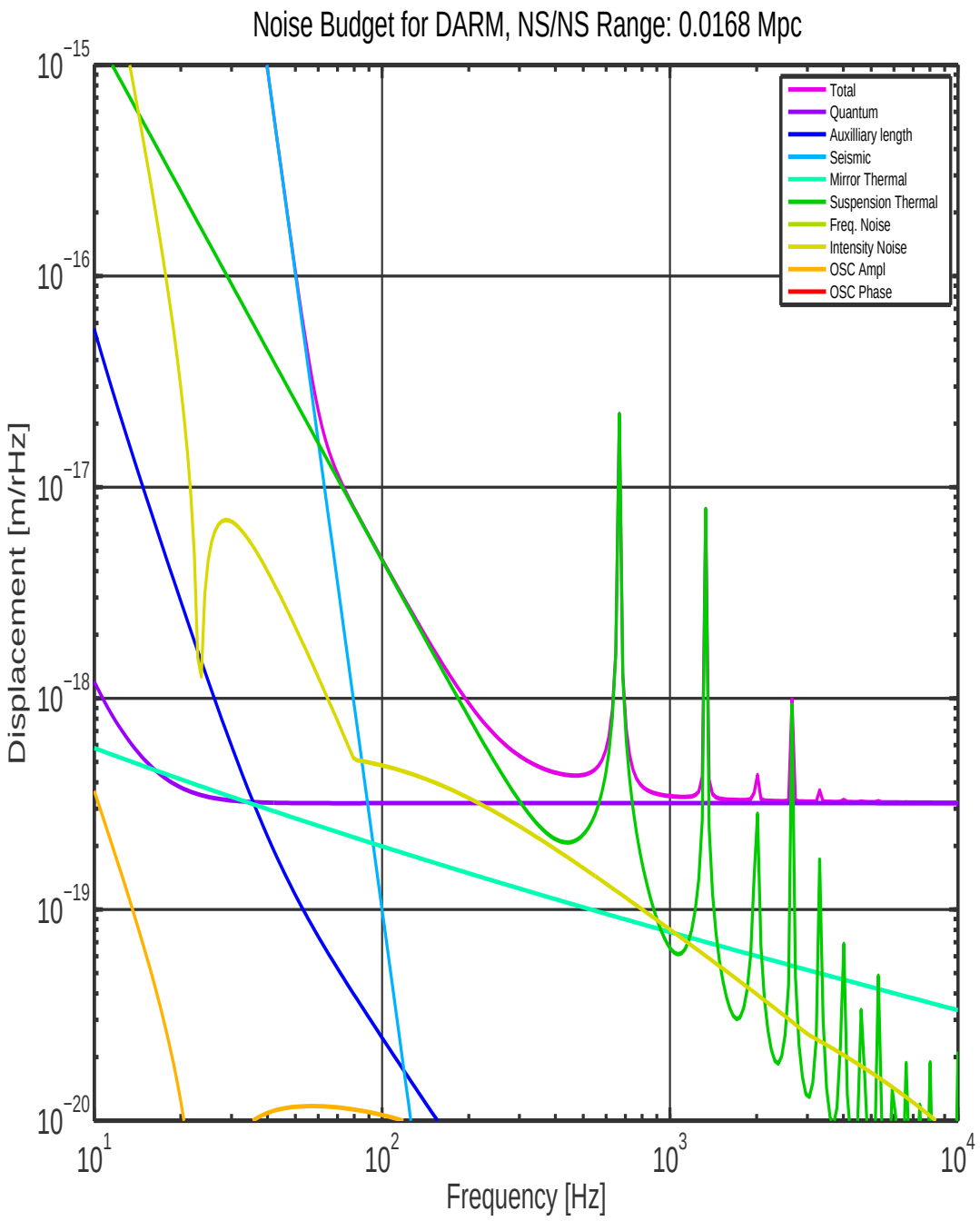

Figure 4: DARM noise budget.

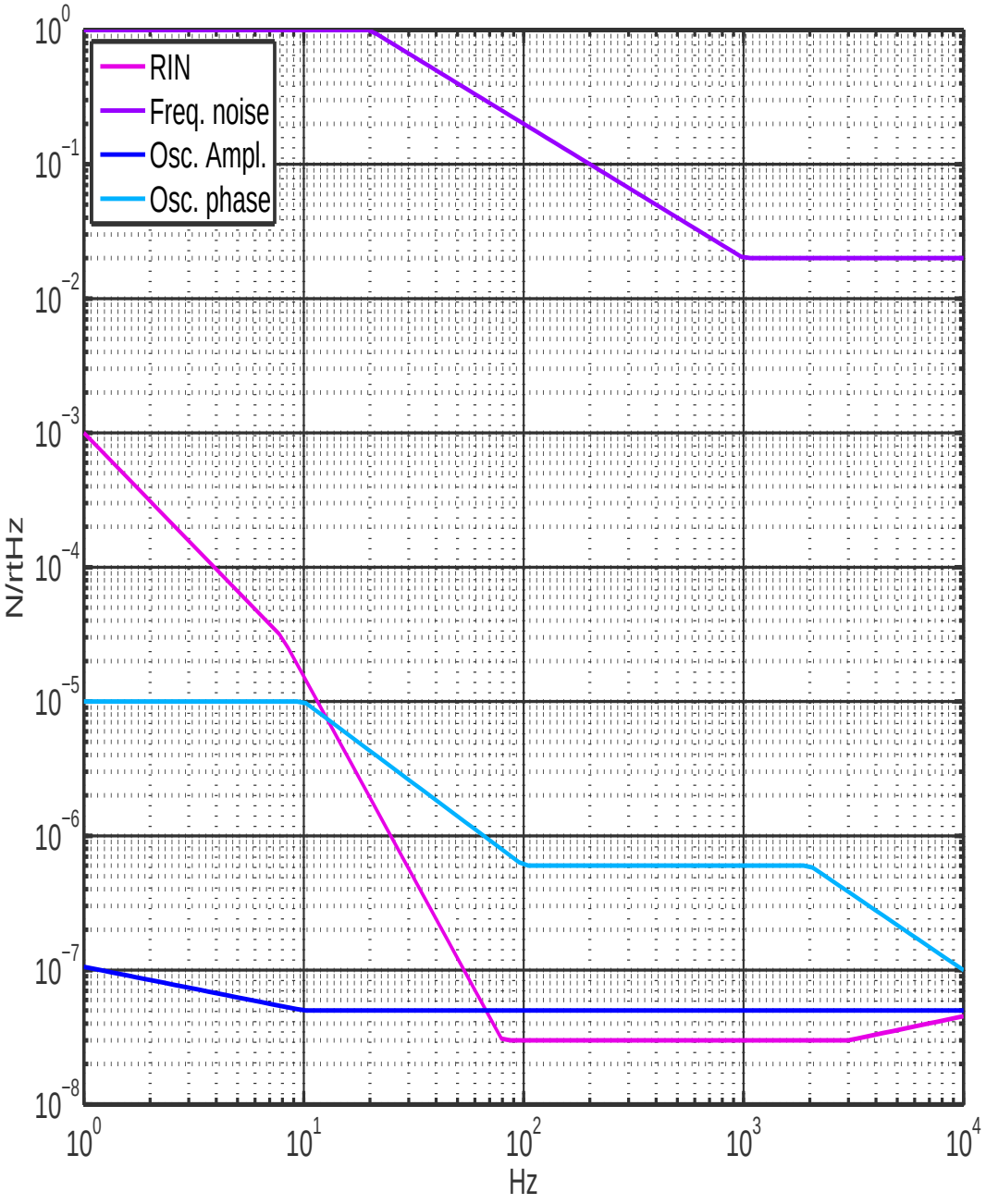

Figure 5: Assumed noise at the IMC input. N = RIN for laser intensity noise, radians for oscillator phase noise, dA/A for oscillator amplitude noise, and Hz for laser frequency noise.

Port	CARM	DARM	PRCL	MICH	SRCL	IMCL
REFL DC	1e+05	5.7e+06	1.4e+04	3.6e+04	4.1e+03	5.4e-05
REFL I1	**1.3e+08**	2.8e+07	1e+07	2.2e+05	**6.9e+04**	0.066
REFL Q1	5.6e+02	4.1e+02	7.1e+04	8.7e+02	1.8e+04	2.9e-07
REFL IM	5.4e+02	**7.8e+04**	**64**	4.8e+02	57	2.8e-07
REFL QM	20	2.9e+03	17	15	1.7	1e-08
REFL IP	5.4e+02	7.8e+04	69	4.7e+02	56	2.8e-07
REFL QP	23	3.4e+03	17	22	2.1	1.2e-08
REFL I2	3.4e+07	7.3e+06	6.1e+06	1.4e+05	2.6e+06	0.017
REFL Q2	2.4e+06	5.3e+05	4.3e+05	2.1e+06	3.6e+02	0.0013
AS DC	1.6e+04	**3.8e+07**	1.6e+03	1.3e+05	3.2e+03	8.4e-06
AS I1	1.7e+02	6.3e+04	31	2.6e+02	5.2	8.9e-08
AS Q1	79	2.9e+04	9.1	23	2.7	4.1e-08
AS IM	0.9	0.2	0.12	0.17	0.0023	4.6e-10
AS QM	1.2	0.27	0.16	0.12	0.0017	6.4e-10
AS IP	0.9	0.2	0.12	0.11	0.0024	4.7e-10
AS QP	1.2	0.28	0.17	0.079	0.0017	6.4e-10
AS I2	1.2e+02	4.4e+04	9.5	2.4e+02	6.3	6.3e-08
AS Q2	3.8e+03	1.4e+06	3e+02	4.9e+03	4.5e+02	2e-06
POX DC	5.9e+03	8.1e+04	5.7e+02	3.9e+02	8.9e+02	3e-06
POX I1	8.7e+05	7e+05	**1.6e+05**	1.3e+03	1.4e+02	0.00045
POX Q1	1.5e+05	1.2e+05	1.3e+04	6.3e+02	23	7.7e-05
POX IM	8.6	7.6	1.1	0.059	0.038	4.4e-09
POX QM	11	9.6	1.4	0.042	0.0064	5.6e-09
POX IP	9.6	8.6	1.3	0.055	0.025	5e-09
POX QP	9.6	8.5	1.2	0.037	0.0058	5e-09
POX I2	4.3e+05	3.5e+05	3.4e+04	6e+02	**4.5e+04**	0.00022
POX Q2	3.2e+05	2.6e+05	**2.5e+04**	**4.6e+04**	5.8e+04	0.00017
POY DC	5.2e+03	7.9e+04	5.1e+02	3.6e+02	1e+03	2.7e-06
POY I1	8.5e+05	5.9e+05	**1.6e+05**	1.2e+03	1.2e+02	0.00044
POY Q1	1.5e+05	1e+05	1.2e+04	9e+02	29	7.5e-05
POY IM	12	6.6	1.6	0.092	0.019	6.4e-09
POY QM	5.4	2.9	0.69	0.012	0.0003	2.8e-09
POY IP	9.6	5.1	1.3	0.091	0.03	5e-09
POY QP	9.8	5.2	1.3	0.044	0.0006	5e-09
POY I2	4.2e+05	3e+05	3.3e+04	6.2e+02	**4.7e+04**	0.00022
POY Q2	3.5e+05	2.5e+05	**2.7e+04**	**4.9e+04**	6e+04	0.00018
POB DC	5.8e+02	8.4e+03	57	37	84	3e-07
POB I1	8.9e+04	6.2e+04	**1.6e+04**	1.3e+02	13	4.6e-05
POB Q1	1.5e+04	1e+04	1.3e+03	61	3.9	7.7e-06
POB IM	1.4	0.74	0.18	0.00044	0.011	7e-10
POB QM	0.4	0.22	0.053	0.0025	3.3e-05	2e-10
POB IP	1.4	0.75	0.18	0.00053	0.011	7.1e-10
POB QP	0.22	0.12	0.03	0.0016	2e-05	1.1e-10
POB I2	4.5e+04	3.1e+04	3.5e+03	62	**4.4e+03**	2.3e-05
POB Q2	3.3e+04	2.3e+04	**2.6e+03**	**4.4e+03**	5.6e+03	1.7e-05
POP DC	86	2.5e+04	10	1.6e+02	18	4.4e-08
POP I1	1.8e+05	3.9e+04	**3.2e+04**	**2.6e+02**	**25**	9.2e-05
POP Q1	2.9e+04	6.4e+03	2.5e+03	49	4.1	1.5e-05
POP IM	0.0069	1.1	0.0045	0.0035	0.005	4e-12
POP QM	0.012	1.6	0.0011	0.0028	0.00076	5.8e-12
POP IP	0.0036	0.7	0.0029	0.0012	0.0048	2.5e-12
POP QP	0.014	1.9	0.0045	0.0035	0.00086	6.6e-12
POP I2	6.7e+04	1.5e+04	5.2e+03	96	**1.2e+04**	3.5e-05
POP Q2	2.2e+03	4.7e+02	**1.7e+02**	**9.2e+03**	**3.9e+02**	1.1e-06

Table 2: Sensing matrix at 100 Hz, with zero-detuning.

Port	CARM	DARM	PRCL	MICH	SRCL	IMCL
REFL DC	1.9e+05	9.5e+05	2.7e+03	2.2e+04	7.3e+02	0.0001
REFL I1	**2.1e+08**	4.1e+04	1e+07	2.8e+05	**6.9e+04**	0.11
REFL Q1	3.7e+03	6.1	7.2e+04	8.7e+02	1.8e+04	1.9e-06
REFL IM	5e+02	**1.3e+04**	**5.9**	2.8e+02	9.3	2.6e-07
REFL QM	45	1.1e+03	16	28	2.6	2.3e-08
REFL IP	5e+02	1.3e+04	9.6	2.8e+02	9.9	2.6e-07
REFL QP	75	1.9e+03	14	41	2.9	3.9e-08
REFL I2	5.5e+07	1.1e+04	2.3e+06	1.7e+05	2.6e+06	0.028
REFL Q2	4e+06	7.4e+03	1.5e+05	2.1e+06	1.5e+02	0.0021
AS DC	2.7e+04	**3.8e+07**	2.6e+03	1.3e+05	32	1.4e-05
AS I1	2.8e+02	6.3e+04	45	2.6e+02	0.18	1.5e-07
AS Q1	1.3e+02	2.9e+04	15	23	0.28	6.7e-08
AS IM	1.5	0.0041	0.02	0.16	0.0025	7.6e-10
AS QM	2	0.0011	0.028	0.12	0.0022	1e-09
AS IP	1.5	0.0047	0.021	0.11	0.0026	7.7e-10
AS QP	2	0.0074	0.028	0.078	0.0023	1.1e-09
AS I2	2e+02	4.4e+04	14	2.4e+02	2.7	1e-07
AS Q2	6.2e+03	1.4e+06	4.1e+02	4.9e+03	3.4e+02	3.2e-06
POX DC	9.1e+03	1.2e+05	8.8e+02	60	9.8e+02	4.7e-06
POX I1	1.4e+06	6.2e+05	**2.4e+05**	1.5e+03	10	0.00074
POX Q1	1.8e+05	8e+04	2.7e+03	4.7e+02	23	9.5e-05
POX IM	17	1.2	0.23	0.03	0.044	8.8e-09
POX QM	15	1.1	0.2	0.008	0.012	7.7e-09
POX IP	19	1.4	0.26	0.022	0.032	1e-08
POX QP	11	0.8	0.15	0.0068	0.0099	5.8e-09
POX I2	7.1e+05	3.1e+05	4.2e+04	95	**4.5e+04**	0.00037
POX Q2	5.2e+05	2.2e+05	**3.1e+04**	**4.5e+04**	5.8e+04	0.00027
POY DC	9.1e+03	1.3e+05	8.9e+02	61	9.6e+02	4.7e-06
POY I1	1.4e+06	6.3e+05	**2.3e+05**	1.2e+03	19	0.00073
POY Q1	1.8e+05	8e+04	2.6e+03	1e+03	26	9.3e-05
POY IM	22	1.5	0.28	0.088	0.02	1.1e-08
POY QM	5.3	0.37	0.068	0.0043	0.006	2.7e-09
POY IP	16	1.1	0.22	0.089	0.028	8.4e-09
POY QP	16	1.1	0.21	0.04	0.012	8.1e-09
POY I2	6.9e+05	3.1e+05	4.1e+04	3.1e+02	**4.7e+04**	0.00035
POY Q2	5.8e+05	2.6e+05	**3.4e+04**	**5e+04**	6e+04	0.0003
POB DC	9e+02	1.3e+04	88	6.1	93	4.7e-07
POB I1	1.5e+05	6.5e+04	**2.4e+04**	1.5e+02	1.1	7.7e-05
POB Q1	1.8e+04	8e+03	2.6e+02	46	2.6	9.5e-06
POB IM	2.2	0.16	0.03	0.00088	0.012	1.2e-09
POB QM	0.61	0.043	0.0088	0.0026	0.00036	3.2e-10
POB IP	2.3	0.16	0.03	0.00096	0.012	1.2e-09
POB QP	0.34	0.024	0.0049	0.0017	0.00018	1.7e-10
POB I2	7.4e+04	3.2e+04	4.5e+03	10	**4.4e+03**	3.8e-05
POB Q2	5.3e+04	2.3e+04	**3.3e+03**	**4.4e+03**	5.6e+03	2.8e-05
POP DC	24	4.2e+03	0.39	95	3.3	1.2e-08
POP I1	2.9e+05	57	**4.7e+04**	**2.8e+02**	**1.3**	0.00015
POP Q1	3.6e+04	7.1	5.3e+02	51	0.5	1.9e-05
POP IM	0.0035	0.12	0.0046	0.0013	0.0044	2.4e-12
POP QM	0.012	0.31	0.0019	0.0037	0.0002	6.2e-12
POP IP	0.00067	0.032	0.004	0.00087	0.0045	6.9e-13
POP QP	0.013	0.33	0.0024	0.0033	0.00021	6.6e-12
POP I2	1.1e+05	21	6.8e+03	17	**1.2e+04**	5.7e-05
POP Q2	4.6e+03	34	**2.7e+02**	**9.2e+03**	**2.8e+02**	2.4e-06

Table 3: Sensing matrix at 1000 Hz, with zero detuning

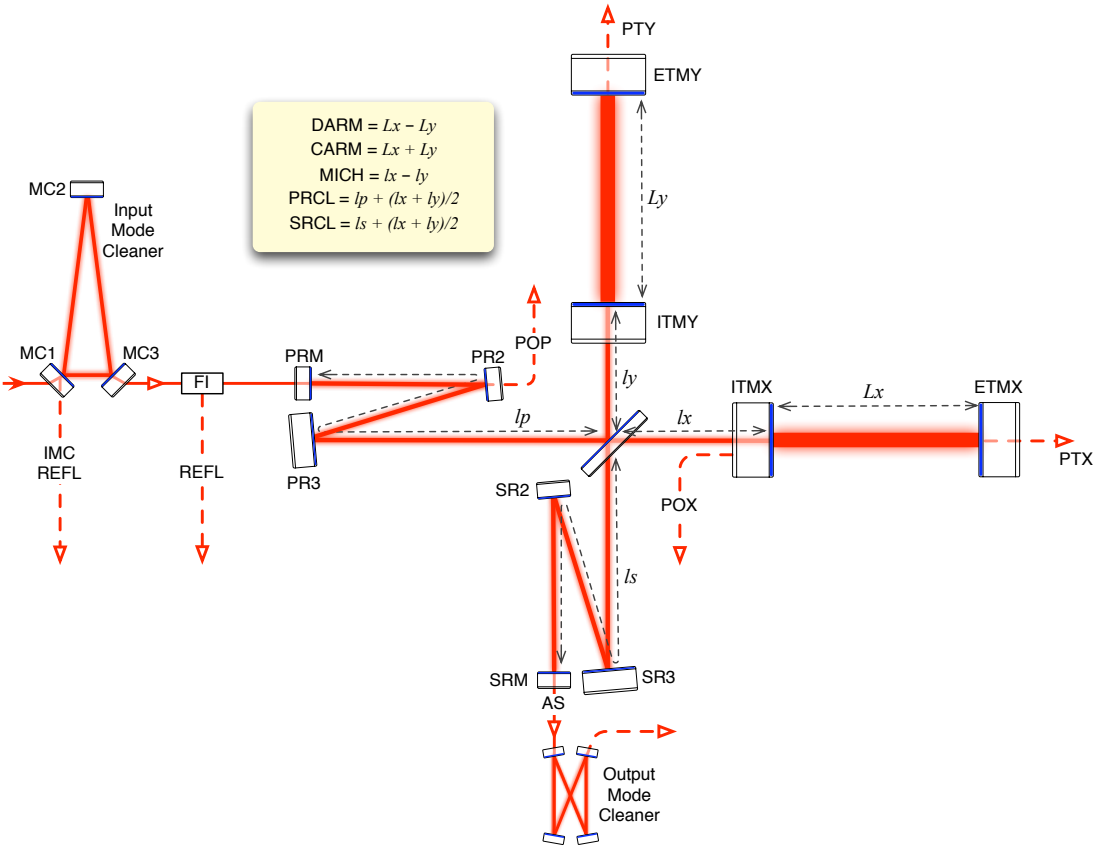

Figure 6: Def of LSC DOFs

The present lock acquisition path at the 40m involves first locking the interferometer with a non-negligible common arm offset which is subsequently reduced to zero in a controlled manner. The first stage of this technique is statistical in nature, and is the most significant contributor to the uncertainty in time required to acquire lock. This technique also introduces complications due to the changing optical plant as the CARM offset is reduced.

We envisage developing an improved version of this path for application to a broadband recycled 40m. Our approach will mirror that covered in section 9 of [3]. However, we do not plan to implement a SPI at the 40m. We shall instead explore the possibilities described in section 4.2.This will involve two parallel investigations:

- Control signals which are not affected by common arm offsets.
- Independent control the arm cavity length at the nanometre level - allows one to hold the arms both on or off resonance and smoothly transition between these states.

We address each in turn:

4.1 Harmonic Demodulation

Simulations by L. Barsotti show that error signals for the central interferometer (PRCL,SRCL & MICH) are available by demodulating the reflected light at $3f_1$ (PRCL, MICH) and $3f_2$ (SRCL)[3]. These signals are attractive as they present little sensitivity to CARM detuning, while avoiding the complexity introduced by doubly demodulating PD outputs.

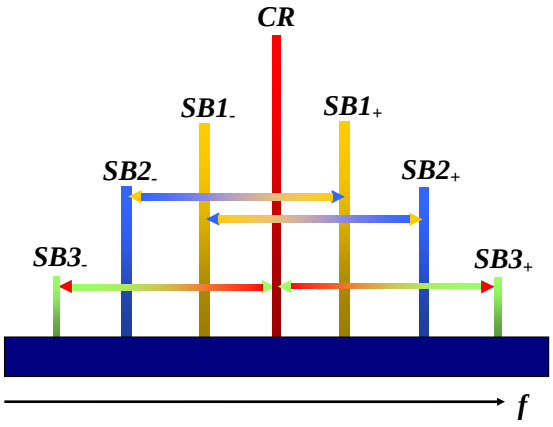

Figure 7: The reflected signal demodulated at $3f_1$ is dominated by the beat between first and second order sidebands.

Consider the case of the $3f_1$ demodulation. These $3f$ signals arise from the beat between the first and second order sidebands ($f_1SB1_{\pm}$ and $f_1SB2_{\mp}$) and between the carrier and third order sidebands (CR and $f_1SB3_{\pm}$) (figure 4.1). The signal from the beat between sidebands is generally much larger than that due to the carrier/$SB3$ beat as the interferometer reflectivity for the third order sidebands is low. In contrast, the second order sidebands are non-resonant in the recycling cavity and hence provide a stable local oscillator in reflection which is almost independent of optical parameters, interferometer resonances and CARM offset. Figure 4.1 shows a comparison between $1f$ and $3f$ signals for various CARM offsets.

Preliminary tests at the 40m using existing electronics have shown that MICH and PRCL can be held on REFL31 (Reflected light demodulated at $3f_1$=99MHz) I & Q, respectively.

4.2 Auxiliary signals

To manipulate the arm cavities independently of the 'standard' control structure we require some means of separating the chosen readout method from the usual PSL light. There exist a number of options:

- **Orthogonal polarizations**

  It is possible to inject orthogonally polarized light through any of the auxiliary ports and distinguish these signals by means of a polarizing beam splitter. To get a wide tuning range with this scheme we would need to use an auxiliary laser and tune its

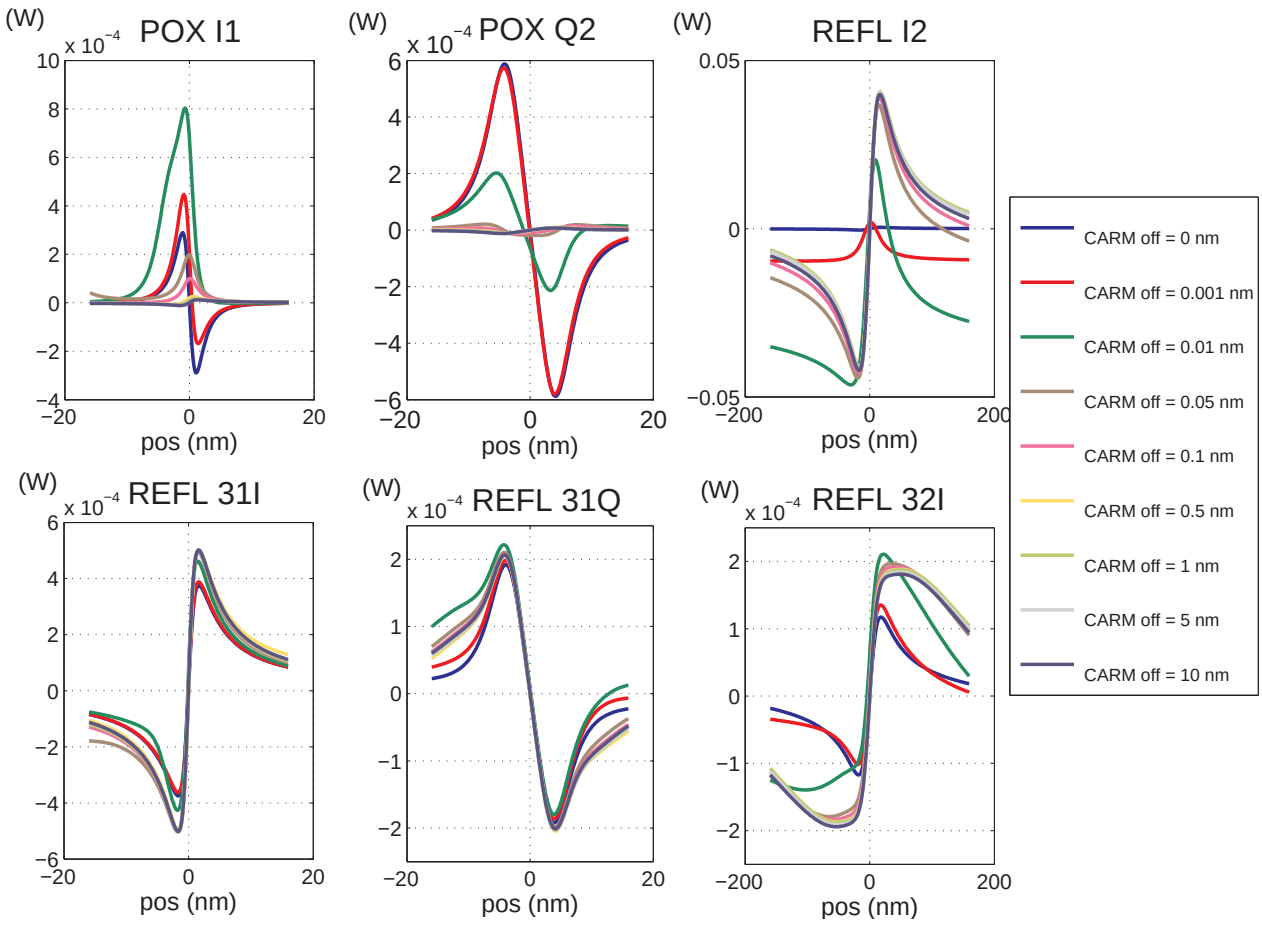

Figure 8: A comparison between (simulated) science mode and lock acquisition signals for various CARM offsets. Left: PRCL, centre - MICH, right - SRCL. Parameters used are representative of AdvLIGO, we expect similar results at the 40m. Reproduced from p. 60 of [3]

frequency by several MHz. This scheme, as well as some of the following, would require the frequency stabilization of an external laser with respect to the PSL beam.

- **Frequency shifted PSL light**

  Better control of the arm length is achievable using a frequency shifted PSL pick-off. The shift would be in the hundreds of MHz regime and would likely be introduced by double-passing an AOM. Adjustment of the frequency shift via a VCO would give a wide tuning range and allow the arm to be swept to a resonance of the PSL light. A very similar scheme would be to use an external, tuneable laser as above.

- **Other wavelengths**

  The use of other wavelengths represents another valid option. A simple choice might be to double the PSL light to 532 nm. This beam benefits from the stabilisation of the PSL pump beam whereas other light sources must be independently stabilised.

  Use of a second wavelength would require dichroic coatings (both HR and AR). Recent

explorations by S. Ballmer suggest that this type of coating can be achieved through small deviations from a 1/8, 3/8 design.

We should also take advantage of the dispersion in the bulk to achieve a split of this other color with respect to the 1064 nm beam.

- **Digital interferometry/ PRN**

  Phase modulated light, imprinted with pseudo random code is, when suitably demodulated, able to determine the positions of optics over a wide range without requiring any resonant phase shifts[21][1]. We do not expect to investigate this technology independently but would like to host outside experiments (ANU).

Having a modulated beam one must decide where to inject it to create useful signals[2]. Two ideas have been proposed:

- **Injecting through ETM** From the ETM side the arm cavities are massively under coupled. This leads to small signal levels which are could easily be dominated by technical noise. Additionally, the light from the arm will enter the central cavities and efforts must be taken to minimize the coupling between the arm signal and other degrees of freedom. In this respect a second wavelength would be advantageous as the dispersion of fused silica may allow the separation of beams from the recycling cavities and the arm if the wedges are of appropriate size and orientation. Note: this wedge trick will not work for AdvLIGO since the beam sizes there are larger; we would have to use a beam reducer to split those beams.

- **Injecting through pick-offs** Similar to the above. Injecting through POX/POY gives an appreciable improvement in the signal to noise ratio since the arm cavities become over coupled with this topology. Coupling to the central interferometer is reduced. POP is also under consideration but is dependent on the layout of the stable recycling cavities.

5 Noise Diagnostics

The following is a non-exhaustive list of diagnostic tests that we will do in order to verify our models of a DRFPMI with DC Readout. As in the past, we expect the most useful parts of the noise coupling measurements to be where we do not find agreement with the Optickle model. Performance requirements for the AdvLIGO system are listed in Section XXX of the ISC CDD [3].

[1] We do not discuss the suspension point interferometer mentioned in this reference as there are no plans to study this idea at the 40m

[2] We are presently considering an actively stabilised fibre distribution system for transporting any secondary light source.[23]

5.1 Sensing and Control System Noise

5.1.1 Beam jitter coupling

Band-limited noise injections on all of the interferometer optics as well as the input beam to the interferometer and the OMC tip/tilt steering mirrors. We will apply this noise in conjunction with low frequency misalignments of the core optics in order to verify our models of bilinear jitter coupling [24].

5.1.2 Auxiliary Length Degrees-of-freedom

The sensing and control of each auxiliary length degree-of-freedom must be done in such a way that limits the coupling of their sensing noise into the GW readout. We will check via standard swept sine tests that the modeled transfer functions are correct and also do a set of Monte-Carlo offset/noise tests as above to check our estimates of allowable loop offsets.

5.1.3 Frequency Stabilization

Due to the short arm cavity lengths, we expect there not be a significant frequency noise coupling in the 40m, even with low light levels on the CARM/CM sensing detector(s). This can be compromised by scattering and clipping noise in the MC/CM sensing chains but this also seems controllable. There are frequency noise injection points available on these servos.

5.1.4 Laser Intensity Noise

Laser intensity stabilization at the $5 \times 10^{-8}/\sqrt{\mathrm{Hz}}$ level which is currently achieved seems copacetic and so we will not pursue an AdvLIGO style Intensity Stabilization Servo (ISS). The existing system has an injection point which can hooked up to the AWG.

5.1.5 Modulation Source Noise

Modulation/Oscillator noise is often tricky to model correctly and diagnose. The baseline plan is to continue with the Marconi (IFR) generators even though they have a much higher phase noise than the Wenzel OCXOs employed in iLIGO and GEO600. The Marconi and the RF AM Stabilization circuit allow high bandwidth modulation and straightforward wideband tuning range which are the *sine qua non* of oscillator noise characterization.

6 DC Readout System

As Advanced LIGO will use the technique known as *DC Readout* [10] for detection of the gravitational wave channel it is a crucial part of the global length sensing and control system, and thus needs to be tested in an integrated manner. The current 40 m has a DC Readout system which consists of:

- A pair of piezo-electric tip-tilt steering mirrors (from Piezo-Jena) at the output port of the interferometer.
- A length adjustable (via New Focus picomotor), fixed mount, mode-matching telescope with spherical mirrors.
- A monolithic, four-mirror mode cleaning cavity with a finesse of 210 and a transmission of approximately 90%. The body is made of copper. The beam waist is 370 microns.
- A pair of bare photodiodes (exposed to the vacuum) with an electronics amplification package housed in a separate canister, all installed in the vacuum system atop a seismic isolation stack.

As of this writing, the DC readout has not been demonstrated with a DR system. The program to study the PRFPMI with DC Readout was extended to support noise modeling for Enhanced LIGO. The system was designed to work with the DRFPMI and it is expected to also work well with the upgraded system. The HOM susceptibility analysis was done assuming the old system with the higher frequency sidebands and so it remains to be determined if the existing low finesse OMC will be sufficient in isolating the DC Readout photodiodes.

As the location and size of the arm cavity beam waist is not expected to change, all the installed components will function in the upgraded 40m interferometer. However, desirable upgrades include, in order of priority:

- **Photodetectors** The currently installed vacuum-compatible DC Readout photodetectors are a first prototype, and improvements have been made to the design for Enhanced LIGO. The 40 m DC Readout system should be updated with a new photodetection chain with electronics similar to that being installed into Enhanced LIGO in order to lower the front end electronics noise. This will require laying out a new board to fit inside the in-vacuum can which currently contains the PD pre-amp.
- **OMC** A new output mode cleaner can be built and installed which matches the finesse of the projected Advanced LIGO output mode cleaner, to provide a more faithful representation. Another option is to swap mirrors to up the finesse of the existing copper OMC. We will wait to do some supporting calculations before going down that road.
- **Tip-Tilts** The piezo-electric steering mirrors can be replaced with suspended tip-tilt mirrors, to more faithfully reproduce the situation in advanced LIGO. Equipping these with curved mirrors could allow the removal of the fixed mode-matching telescope. The baseline plan is to stay with the PZT mirrors.

7 Squeezed Light Injection

The 40m upgrade will allow for squeezed light/vacuum injection through the dark port via the AS port Faraday Isolator. At this time we do not include the design of such a squeezer but just leave the port open in case future squeezed light research indicates a need for this kind of work.

8 Adaptive Noise Cancellation

Recent work [26] has shown that there is some promise in exploring active cancellation of environmental noise sources. The concomitant technique of adaptive filtering has recently [25] been demonstrated on a real time system in the 40m lab.

In order to pursue this we will have a dedicated front end system acquire many signals including the PEM and SUS/ASC sensors. Some of the envisioned development includes:

- **Seismic** Using the ultra-low frequency Wilcoxon accelerometers as well as a few seismometers (Ranger SS-1, Guralp CMG-40T, etc.) we will send signals to the longitudinal (POS) input of the suspensions to minimize fringe velocities for ease of lock acquisition. This will not lower the overall control signal amplitudes at the 40m nor reduce the amount of angular fluctuation but should ease locking efforts during the daytime.

  From our modeling we expect that optic angular fluctuations at the 40m and in AdvLIGO are dominated by length to angle cross-coupling in the suspensions and so it is not likely to be useful to attempt feed-forward cancellation of tilt at the 40m (although it should be useful for the AdvLIGO SEI system).

- **Acoustic** To explore higher frequency noise cancellation and reduce the noise in the 100-1000 Hz band, we will install a set of microphones in the LSC sensing tables and the PSL and attempt to cancel some of the observed scattering/clipping noises. All of the ISC beam paths in AdvLIGO will be in-vacuum to avoid this effect but the technique may be useful to reduce unexpected couplings.

- **Magnetic** A set of magnetometers (Bartington or otherwise) will be installed to attempt subtraction of power line harmonics picked up in the sensing channels and from pickup in the test mass magnets. In AdvLIGO this technique may be useful to cancel pickup in the PUM (PenUltimate Mass) of the quad suspensions and the actual mirror of the triple suspensions of the beamsplitter and recycling cavity suspensions. Direct hardware based subtraction may reduce the bilinear noise which masks the Crab pulsar signal in iLIGO.

- **RF** A more speculative source of excess noise is direct coupling of RFI at the LSC modulation frequencies into the readout electronics. RF antennae with modulators/demodulators will be installed to explore noise cancellation via this mechanism.

- **LSC Corr** A potentially significant noise limit in AdvLIGO may be feedthrough of sensing noise from the aux. length loops. In order to achieve large cancellation factors of this noise we may be forced to use adaptive noise cancellation. We will build this into the LSC system at the 40m either directly or by hooking in a parallel process running the adaptive code.

The total list of sensors is still being determined but is likely to include a seismometer, several accelerometers, microphones, magnetometers, and RF antennae. We will use the existing PEM and PSL/IOO ADCU systems to acquire the slow channels. For all of the

~100 Hz BW cancellation we will require ADCs with less delay than the ICS-110B and therefore would hook into the new acquisition system with General Standards ADCs.

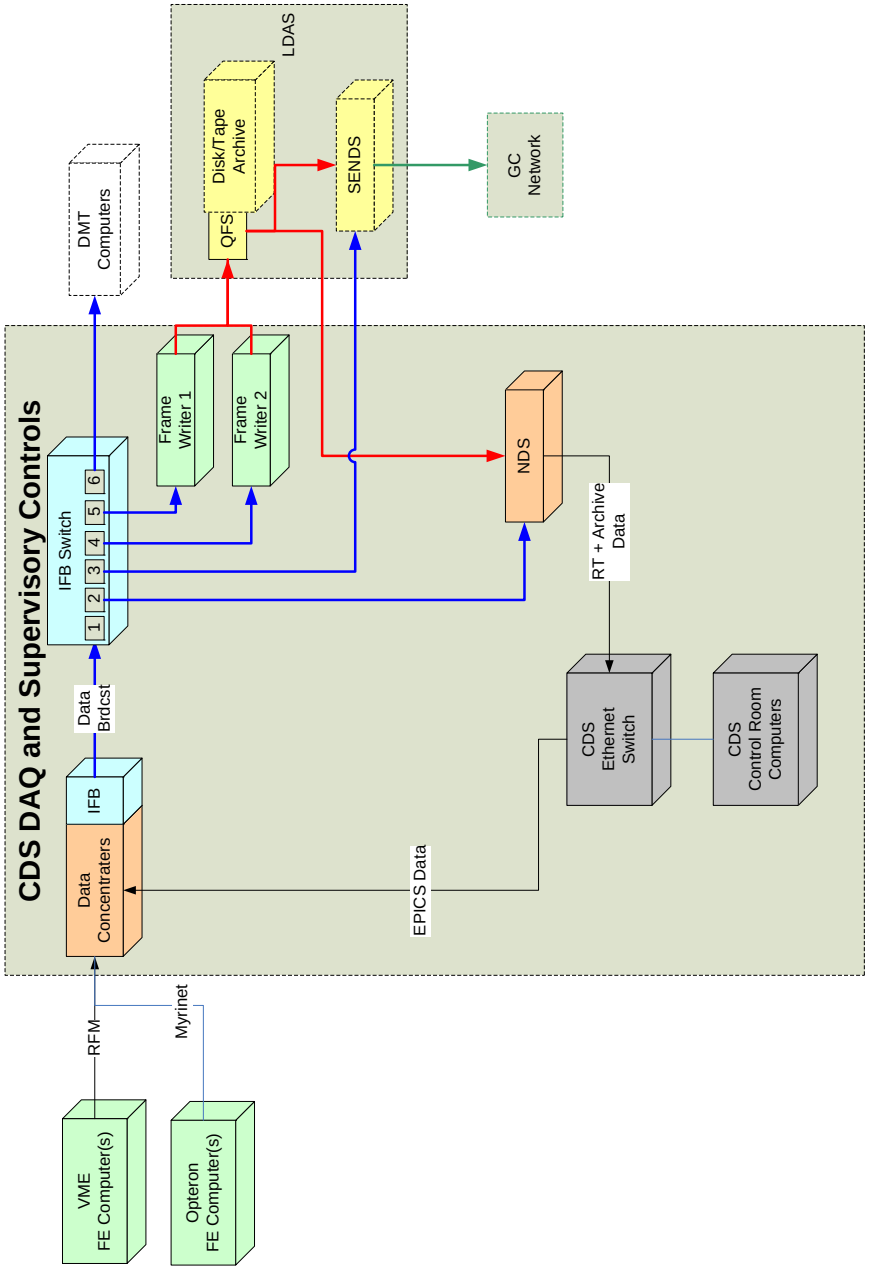

Figure 9: DAQ and Controls Diagram

References

[1] LIGO, "Advanced LIGO Wiki", http://ilog.ligo-wa.caltech.edu:7285/advligo/AdvLigo

[2] ISC Group, "Interferometer Sensing and Control Requirements", http://www.ligo.caltech.edu/docs/T/T070236-00.pdf

[3] ISC Group, "Interferometer Sensing and Control Conceptual Design", http://www.ligo.caltech.edu/docs/T/T070247-00.pdf

[4] R. Adhikari, S. Ballmer, M. Evans, P. Fritschel, "Arm Cavity Finesse For Advanced LIGO", http://www.ligo.caltech.edu/docs/T/T070303-1.pdf

[5] B. Abbott *et al.*, "Conceptual Design of the 40 meter Laboratory Upgrade for prototyping a Advanced LIGO Interferometer", T010115, http://www.ligo.caltech.edu/docs/T/T010115-00.pdf

[6] B. Barr *et al.*, "Control sideband generation for dual-recycled laser interferometric gravitational wave detectors", Class. Quantum Grav. 23 (2006) 5661, http://www.ligo.caltech.edu/docs/P/P060022-02

[7] O. Miyakawa *et al.*, "Measurement of Optical Response of a Detuned Resonant Sideband Extraction Interferometer", Phys.Rev.D74, 022001 (2006), http://www.ligo.caltech.edu/docs/P/P060007-01.pdf

[8] R. Ward *et al.*, "DC Readout Experiment at the Caltech 40m Prototype Interferometer", http://www.ligo.caltech.edu/docs/ScienceDocs/P/P070125-00.pdf

[9] A. Lazzarini and R. Weiss, "LIGO Science Requirements Document", http://www.ligo.caltech.edu/docs/E/E950018-02.pdf

[10] P. Fritschel, "DC Readout for Advanced LIGO", http://ilog.ligo-wa.caltech.edu:7285/advligo/AdvLigo

[11] http://lhocds.ligo-wa.caltech.edu:8000/mLIGO/Nonlinearity_of_the_DC_readout_signal

[12] R. Adhikari, "Sensitivity and Noise", http://www.ligo.caltech.edu/docs/P/P040032-00.pdf

[13] S. Ballmer, "LIGO Interferometer Operating as a Radiometer", http://www.ligo.caltech.edu/docs/P/P060043-00.pdf

[14] K. McKenzie, "Mode Cleaner Length Measurement", http://tinyurl.com/2ubeac

[15] V. Frolov, "RFAM of the RF stabilization box is measured", http://tinyurl.com/4rkq6d

[16] D. Sigg and J. Sidles, "Optical Torques in Suspended Fabry-Perot Cavities", http://www.ligo.caltech.edu/docs/P/P030055-C/

[17] ISC Group, "Length Sensing and Control Final Design (iLIGO)", http://www.ligo.caltech.edu/docs/T/T980068-00.pdf

[18] P. Fritschel, "LIGO", http://arxiv.org/abs/0711.3041

[19] M. Evans, "Optickle", http://www.ligo.caltech.edu/docs/T/T070260-00.pdf

[20] M. Evans, "Optickle (LSC talk)", http://www.ligo.caltech.edu/docs/G/G070728-00

[21] B. Slagmolen et al., "Adv. LIGO Arm Cavity Pre-Lock Acquisition System", AdvLIGO Wiki, SPI page, http://lhocds.ligo-wa.caltech.edu:8000/advligo/

[22] O. Miyakawa et. al., "Mach-Zehnder interferometer for Advanced-LIGO optical configurations to eliminate sidebands of sidebands", http://www.ligo.caltech.edu/docs/T/T040119-00.pdf

[23] S.M. Foreman et al, "Remote transfer of ultrastable frequency references via fiber networks", Review of Scientific Instruments 78, 021101/1-25 (2007).

[24] D. Sigg et. al., "Modal Model Update 10: Noise Coupling and Random Imperfections", http://www.ligo.caltech.edu/docs/T/T980001-00.pdf

[25] M. Evans, R. Adhikari, "Adaptive Noise Cancellation (LSC talk)", http://www.ligo.caltech.edu/docs/G/G080213-00

[26] K. Pepper, "Newtonian Noise Simulation and Suppression for Gravitational Wave Interferometers (SURF Report)", http://www.ligo.caltech.edu/docs/T/T070192-00/

[27] R. Weiss, "Electromagnetically Coupled Broadband Gravitational Antenna", http://www.ligo.caltech.edu/docs/P/P720002-01

A New Interferometer Parameters

ITM Transmission	0.014
PRM Transmission	0.07
SRM Transmission	0.07
ITM imbalance ($T_{ITMX} - T_{ITMY}$)	$T_{ITM}/50$
Average round trip arm loss	160 ppm
Differential arm loss	50 ppm
Beamsplitter R/T imbalance	$\pm 5 \times 10^{-3}$
Differential arm offset from dark fringe	40 pm
Arm Cavity finesse	446
Output mode cleaner finesse	250
Power Recycling cavity length	8.328 m
Signal Recycling cavity length	6.662 m
Schnupp Asymmetry	0.05 m

Table 4: Parameters used in the Optickle modeling. Shown are those parameters that determine the laser and modulation source noise couplings.

B Current (2007) Interferometer Parameters

ITM Transmission	0.005
PRM Transmission	0.07
SRM Transmission	0.07
ITM imbalance ($T_{ITMX} - T_{ITMY}$)	$T_{ITM}/11$
Average round trip arm loss	160 ppm
Differential arm loss	20 ppm
Beamsplitter R/T imbalance	$\pm 5 \times 10^{-3}$
Differential arm offset from dark fringe	25 pm
Output mode cleaner finesse	210
Input mode cleaner finesse	1500
Input mode cleaner length	13.547 m
Power Recycling cavity length	2.15 m
Signal Recycling cavity length	2.257 m
Schnupp Asymmetry	0.452 m

Table 5: Measured parameters of the 40m interferometer as of March 2008. Shown are those parameters that determine the laser and modulation source noise couplings.

C Interferometer Displacement Noise Spectrum

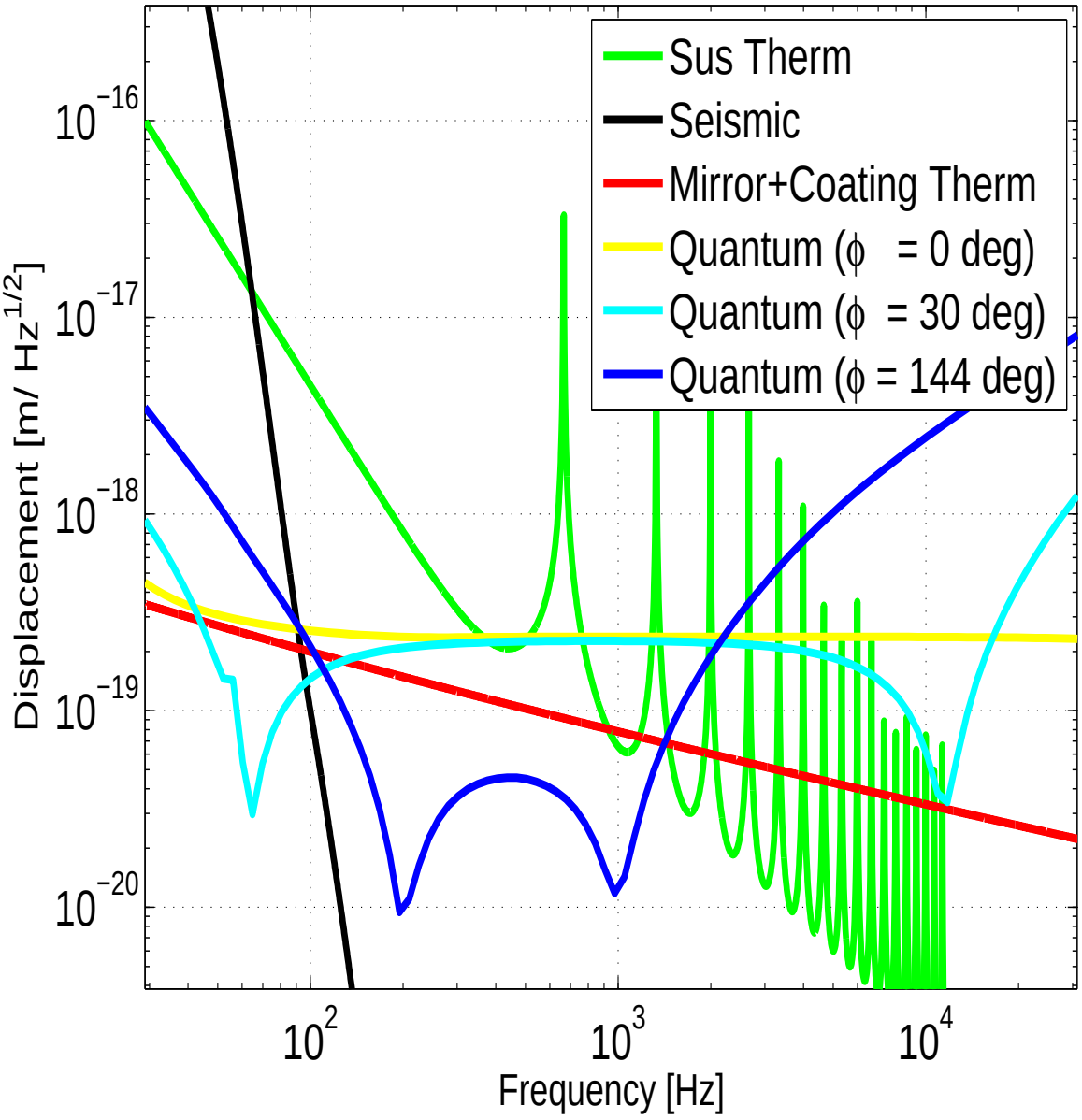

Figure 10: Displacement noise from the 40m Bench model (in the ISC Modeling CVS). The quantum noise is shown for broadband and detuned RSE cases.

D Background and Motivation

Throughout the 1990's, the 40m interferometer was used for developing and testing elements of the Initial LIGO optical configuration and control scheme. It was upgraded in 2001 - 2004 in order to test elements of the (then conceived) Advanced LIGO optical configuration and control scheme, as described in the "Conceptual Design of the 40 meter Laboratory Upgrade for prototyping a Advanced LIGO Interferometer", T010115 [5]. The main parameters of that upgrade are given in Appendix B.

The main goals of that upgrade were to learn how to control a power-recycled Fabry-Perot Michelson (PRFPMI) suspended mass interferometer with a signal recycling cavity (SRC) operated in detuned resonant sideband subtraction mode (RSE, forming a dual-recycled FPMI, DRFPI) (see Appendix C of [5]). The Advanced LIGO design at the time called for the following innovations in optical configuration and control: (a) High finesse arm cavities ($\sim$1200) in order to reduce the power required to circulate in the power recycling cavity. (b) RSE to recover the high-frequency signal response of the detector, "detuned" to optimize it for detection of binary neutron star inspirals in the presence of other technical noise sources. (c) A signal extraction scheme for controlling the DRFPMI that employed a moderate Schnupp asymmetry and two pairs of RF sidebands with very different frequencies, in order to provide the best contrast between the PRC and SRC length degrees of freedom (9 MHz and 180 MHz for AdvLIGO, and 33 MHz and 166 MHz for the 40m testbed, employing "double-demod" signals derived from the sidebands alone to control the DRMI). (d) A Mach-Zehnder to apply both pairs of sidebands in parallel, eliminating "sidebands on sidebands" [6]. (e) DC readout for homodyne detection of the GW signal using arm-filtered carrier light as the local oscillator.

By the end of 2005, the 40m team was able to acquire lock and control all five degrees of freedom of the DRFPMI, in detuned RSE [7]. By 2007, DC readout was demonstrated on a PRFPMI [8].

In the process, several issues were encountered: (a) lock acquisition and control of high-finesse arm cavities is very difficult, requiring the development of many tricks to get robust signals during lock acquisition. (b) The detuned signal cavity formed an optical spring which complicated the dynamics of lock acquisition. (c) High-frequency RF (greater than say, 50 MHz) is hard to work with. (d) Double-demod signals have poor SNR and the demod phases seem to drift around excessively without obvious explanations. (e) The Mach-Zehnder solution proved to have its own problems: intensity noise and non-stationary RFAM. (f) The VME-based control electronics architecture is a liability just as it is for initial LIGO.

Partially in response to these observations, the AdvLIGO ISC group reconsidered high-finesse arm cavities [4], signal extraction schemes that make use of lower RF sideband frequencies [3], and continuing with serial modulation as in initial LIGO.

It will be important to test this new scheme with a realistic, suspended interferometer. The 40m lab is a near-ideal place to do this.

Parameter	40m (1998)	LIGO 4K	40m(2002)	Adv LIGO	units
Carrier λ	514.5	1064.	1064.	1064.	nm
Transmissivity T(ETM)	1.2E-5	1.5E-5	1.0E-5	1.0E-5	
Transmissivity T(ITM)	0.00565	0.02995	0.005	0.005	
Transmissivity T(RM)	0.1375	0.0244	0.07	0.07	
Mode cleaner length	1.0	12.255	13.542	16.655	m
FSR_{MC}	150.	12.23	11.07	9.00	MHz
RF freq1 $f_1 = n_1 fsr_{mc}$	32.7	24.46	33.207	9.00	MHz
Arm Cavity L_{arm}	38.25	3999.	38.55	3999.	m
PR Cavity L_{PRC}	2.294	9.191	2.257	8.328	m
PRM–BS length	0.25	4.396	0.30	4.000	m
BS–ITMinline length	2.315	4.877	2.183	4.536	m
BS–ITMperpin length	1.773	4.599	1.731	4.119	m
Schnupp Asymmetry length	0.542	0.278	0.451	0.416	m
Arm cavity pole freq	1814	91	1578	15	Hz
Arm Cavity Finesse	1080	205	1235	1235	
Rec Cavity Finesse	24	138	47	47	
Arm Cavity power gain	670	130	775	775	
Rec Cavity power gain	9	48	16.5	16.5	
mirror diameter	10.16	25.0	12.5	31.4	cm
mirror length	8.89	10.0	5.0	13.0	cm
mirror mass	1.58	10.8	1.35	40.0	kg
PRM ROC	flat	8700	348	8700	m
ITM ROC	flat	14540	flat	14540	m
ETM ROC	61	7400	57.375	7400	m
n_1	-	3	3	1	
n_2	0	1	0	0	
n_3	7.84	652.13	8.05	239.61	
n_4			0	0	
n_5			5	21	
RF freq2 $f_2 = n_4 f_1$			166.033	180.0	MHz
SR Cavity L_{SRC}			2.151	9.148	m
SRM–BS length			0.200	3.821	m
RSE peak frequency			4000	300	Hz
Signal Cavity tune			0.235	0.038	rad/(π/2)
SRM ROC			365	9000	m

Table 6: Historical comparison of several interferometers' design parameters: the 40m in 1998 (recycling experiment), the Initial LIGO 4K interferometers, the 40m in 2002 (dual recycling for Advanced LIGO), and the Advanced LIGO design circa 2002.